Metal–Organic Frameworks

DOI: 10.1002/anie.201202925

Reversible Interpenetration in a Metal–Organic Framework Triggered by Ligand Removal and Addition**

*Sang Beom Choi, Hiroyasu Furukawa, Hye Jin Nam, Duk-Young Jung, Young Ho Jhon, Allan Walton, David Book, Michael O'Keeffe, Omar M. Yaghi, and Jaheon Kim**

Interpenetration is known for the structures of many minerals and ice;[1] most notably for ice, it exists in doubly interpenetrating (VI, VII, and VIII) and non-interpenetrating (I_h) forms with the latter being porous and having nearly half of the density of the former.[2] In synthetic materials, specifically in metal–organic frameworks (MOFs), interpenetration is generally considered undesirable because it reduces porosity.[3] However, on the contrary, many advantageous properties also arise when MOFs are interpenetrated, such as selective guest capture,[3a] stepwise gas adsorption,[4e] enhanced framework robustness,[5] photoluminescence control,[6] and guest-responsive porosity.[7] Therefore, various strategies have been suggested to control interpenetration during synthesis.[4] However, once these extended network materials are prepared as interpenetrating or non-interpenetrating structures, the degree of interpenetration generally remains unchanged, because numerous chemical bonds must be broken and subsequently reformed in a very concerted way during the process unlike some interlocked coordination compounds in solution (Figure 1 a).[8]

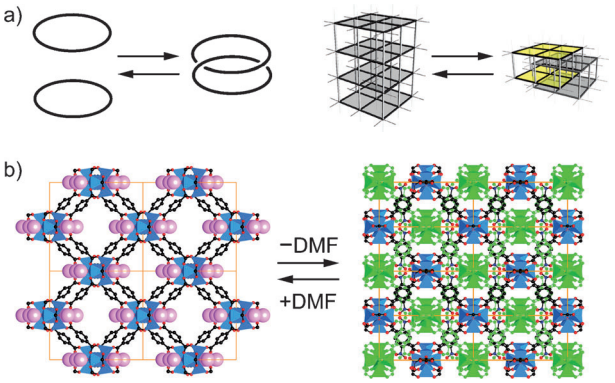

Figure 1. a) Catenation and decatenation processes in molecules (left) are observed in three-dimensional MOFs (right), which can be termed interpenetration and deinterpenetration. b) MOF-123 is converted into the interpenetrating crystals of MOF-246 by the removal of coordinated DMF (large pink spheres). C black, N blue, O red, Zn blue polyhedra. The interpenetrated framework is shown in green.

Some extended structures, such as $[(ZnX_2)_3(\text{tris-(4-pyridyl)triazine})_2]_n$ (X = Cl, Br, I) are known to show framework interpenetration by heat treatments via amorphous intermediate phases.[9] In contrast to this irreversible phase transformation, $[Ag_6Cl(\text{3-amino-1,2,4-triazolate})_4]OH{\cdot}6H_2O$ shows a reversible change in the degree of interpenetration between five-fold and six-fold interpenetration.[10] However, it has not been observed so far that extended structures behave like discrete molecular systems exhibiting full and reversible catenation. Herein, we report that the removal of DMF ligands protruding into the small channels of a three-dimensional metal–organic framework, $[Zn_7O_2(NBD)_5(DMF)_2]$ (MOF-123; NBD = 2-nitrobenzene-1,4-dicarboxylate, DMF = *N*,*N*-dimethylformamide) triggers the transformation of this MOF to a doubly interpenetrating form, MOF-246, $[Zn_7O_2(NBD)_5]$, whose crystal structure is identical to the backbone of MOF-123. Moreover, addition of DMF to MOF-246 results in the reverse transformation to give MOF-123 (Figure 1 b).

Solvothermal reactions between $Zn(NO_3)_2{\cdot}6H_2O$ and H_2NBD in a mixed solution of DMF/methanol produced crystals of MOF-123, the framework of which is formulated as $[Zn_7O_2(NBD)_5(DMF)_2]$. The crystal structure shows that in the heptanuclear inorganic secondary building unit (SBU, $[Zn_7O_2(CO_2)_{10}(DMF)_2]$), which shares a structural similarity with zinc benzoate complexes,[11] $[Zn_7O_2(\text{2,6-difluorobenzoa-}$

[*] S. B. Choi, Dr. Y. H. Jhon, Prof. J. Kim
Department of Chemistry, Soongsil University
Seoul 156-743 (Korea)
E-mail: jaheon@ssu.ac.kr
Dr. H. Furukawa, Prof. O. M. Yaghi
Department of Chemistry, University of California, and
The Molecular Foundry, Lawrence Berkeley National Laboratory
Berkeley, CA 94720 (USA)
Dr. H. J. Nam, Prof. D.-Y. Jung
Department of Chemistry, Institute of Basic Sciences and Sungkyunkwan Advanced Institute of Nanotechnology
Sungkyunkwan University, Suwon 440-746 (Korea)
Dr. A. Walton, Dr. D. Book
School of Metallurgy and Materials, University of Birmingham
Birmingham B15 2TT (UK)
Prof. M. O'Keeffe
Department of Chemistry and Biochemistry
Arizona State University, Tempe, AZ 85287 (USA)
Prof. O. M. Yaghi
Center for Global Mentoring, Graduate School of EEWS (WCU),
Korea Advanced Institute of Science and Technology (KAIST)
Daejeon 305-701 (Korea)

[**] This work is supported by the Hydrogen Energy R&D Center, one of the 21st Century Frontier R&D Programs (the Ministry of Education, Science and Technology of Korea to J.K.). We thank Jihye Yoon and Yoon Jeong Kim for their experimental support, and Dr. Seung-Hoon Choi (Insilicotech Co. Ltd.), Prof. Kimoon Kim (POSTECH), Dr. Hexiang Deng, Kyle Cordova (UC Berkeley), and Dr. Carolyn B. Knobler (UCLA) for their valuable comments.

Supporting information for this article is available on the WWW under http://dx.doi.org/10.1002/anie.201202925.

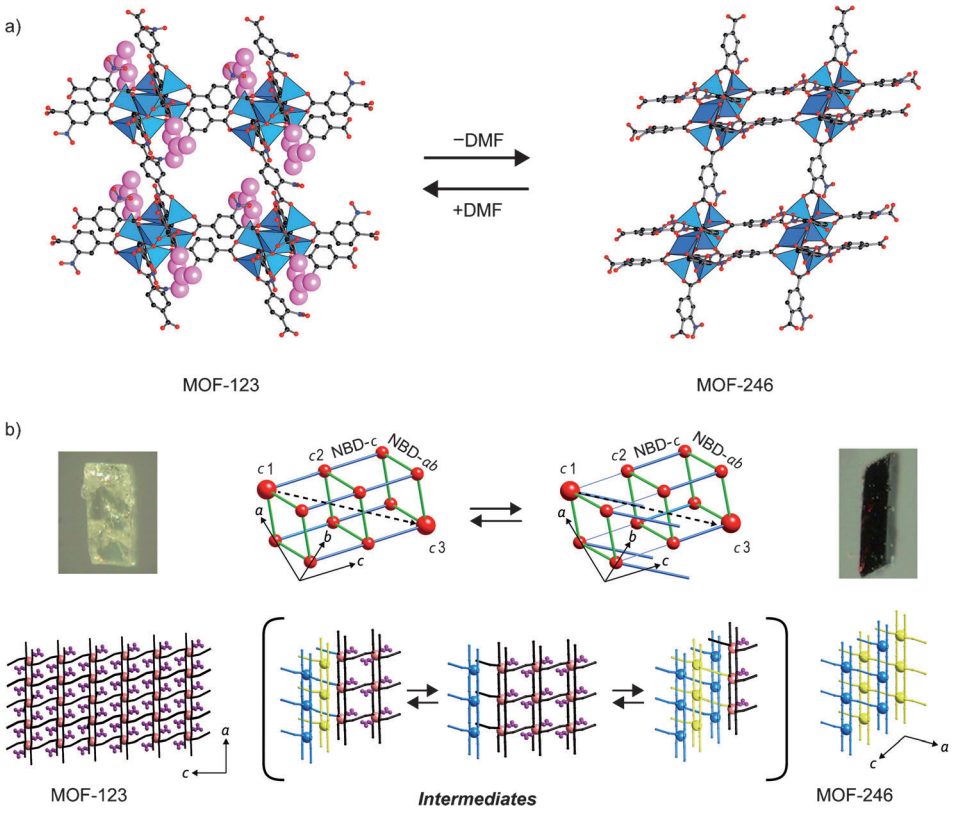

Figure 2. a) Crystal structure of MOF-123 and MOF-246. Only a single framework of MOF-246 is shown for clarity. DMF molecules are shown as pink spheres in MOF-123. C black, N blue, O red, Zn blue polyhedra. Note the rotation of the phenylene rings in the NBD-*ab* linkers that connect inorganic clusters in pairs. b) A proposed transformation mechanism is depicted with ball-and-stick models. Upon DMF removal, framework interpenetration may happen along the crystallographic *c*-axis of MOF-123 at both sides. In the reverse reaction, deinterpenetration, DMF molecules are incorporated to generate MOF-123. The optical images of MOF-123 and MOF-246 are also shown for comparison of their shapes and dimensions.

te)$_{10}$(L)$_2$], where L is tetrahydrofuran or acetonitrile,[12] the two DMF molecules are the terminal ligands on two different Zn centers that protrude into the pores (Figure 2a). The SBUs are joined by ten NBD linkers to give the **fqr** net.[13] This net is in turn derived from a decoration of the primitive cubic (**pcu**) net, which is particularly favorable for the formation of interpenetrating structures;[13] four paired NBD linkers in the crystallographic *ab* plane (termed NBD-*ab*) form double 4.8^2 layers that are connected by NBD linkers along the *c*-axis (NBD-*c*). The framework provides a three-dimensional pore that contains six free DMF molecules per formula unit; its window sizes are ca. 6.7 × 7.8, 3.3 × 6.4, and 3.3 × 6.4 Å along the [001], [110], and [1$\bar{1}$0] directions, respectively. Thermal gravimetric analysis (TGA) of the as-synthesized MOF-123 indicates that both free and coordinated DMF molecules are removed completely below 270 °C, and no further weight loss was observed up to 380 °C (Supporting Information, Figure S1). The structure of the heated crystals (MOF-246) could be determined by a single crystal X-ray diffraction analysis.[10] Crystal structure showed that the removal of the coordinating DMF molecules effected the coordination fashion of the Zn atoms in MOF-246 in a noticeably different fashion from those of MOF-123. In particular, the central Zn atom becomes four-coordinate, whereas it was six-coordinated in MOF-123. The change in the coordination geometry of the Zn atoms accompanied elongation of the SBU shape compared to the SBU shape in MOF-123. Most of all, MOF-246 had two independent frameworks interpenetrated (related by a single translation [0,0,1] of 9.83 Å), while their backbone connectivity is identical to that of MOF-123 (Figure 2). The interpenetration observed here is of Class Ia with single full interpenetration vectors corresponding to the vector [0,0,1] exactly the direction *c*1–*c*3 in Figure 2b.[1] A single framework of MOF-246 has the window sizes of about 4.9 × 4.9, 6.0 × 8.3, and 6.0 × 8.3 Å, which is enough to accommodate the second framework to generate maximal displacement of the interpenetrated nets.

The transformation between these two MOFs was also evidenced by the change in observed crystal volume. Examination of a selected crystal of MOF-123 by optical microscopy shows its rectangular plate morphology with approximate dimensions of 411 × 219 × 180 μm (length × width × thickness); however, when heated to 300 °C, the crystal contracted by about 50 % in its thickness (94 μm), but almost not at all in their length and width (Figure 2b; Supporting Information, Figure S9). This is in agreement with the expected change based on the unit cell parameters and structures of the two MOFs.

Variable-temperature powder X-ray diffraction (PXRD) patterns indicated that MOF-123 undergoes structural changes to produce a new phase via intermediates (Figure 3a). Upon heating MOF-123 crystals, the diffraction intensity corresponding to (001) and (110) crystallographic planes at 6.2° and 6.9°, respectively, in 2θ gradually decreased, and new peaks at 7.9°, 9.7°, and 10.3° started to appear more prominently at 140 °C. This pattern continued to 270 °C, which suggests that the intermediates are comprised of MOF-123 and a new phase in various ratios. The profile of the PXRD patterns did not show any evidence of MOF-123 upon further heating up to 320 °C, indicating completion of the transformation into a new phase, the structure of which is drastically different from the starting component, MOF-123. It is noteworthy that the temperature range of the trans-

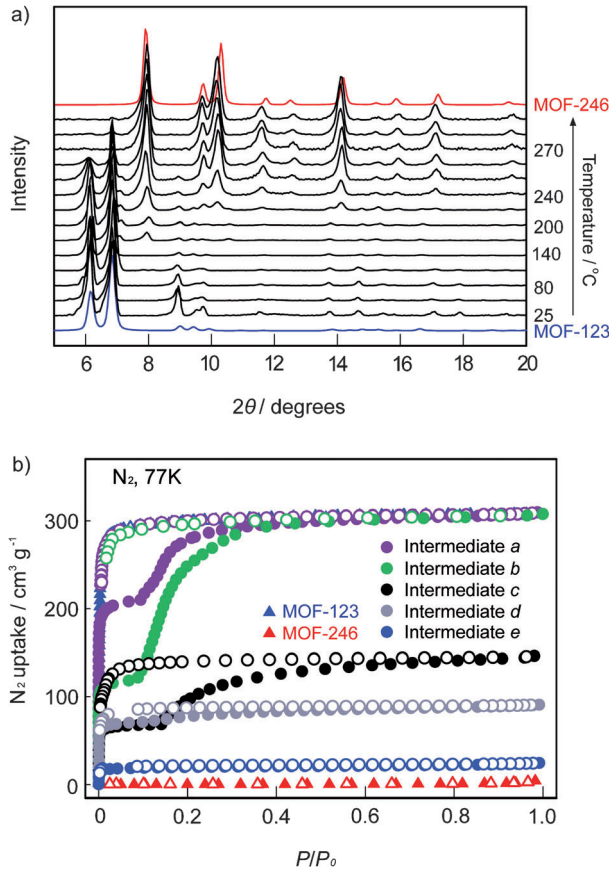

Figure 3. a) PXRD patterns for the interpenetration along with the heating temperatures. b) N_2 adsorption isotherms measured at 77 K for the samples, MOF-123, intermediates (*a* to *e*), and MOF-246. The samples have been prepared by heating MOF-123 at *a*) 70, *b*) 90, *c*) 140, *d*) 180, *e*) 220, and 260 °C under vacuum.

formation is directly correlated with the observed weight loss shown by the TGA analysis.

Based on these observations, it can be possible to propose a plausible mechanism for the transition. Through the liberation of DMF, the Zn_7O_2 coordination sphere should be distorted to some extent. As NBD-*c* linkers in between two Zn_7O_2 units are slightly bent in MOF-123, such distortion can initiate the bond breaking at one end of the NBD-*c* linker (Figure 2b). If half of the NBD-*c* linkers are dissociated to the Zn_7O_2 units, it is possible that the *ab* plane layer slides into the pore of the neighboring layer to reduce the empty space. However, it is not always necessary that the interpenetration starts from both opposite crystal surfaces and complete the transformation at the middle of the crystal. We further believe that the crystal contains many microdomains, each of which shows the transformation. In the case of the reverse reaction, the deinterpenetration starts from the crystal surface, because the pore diameter of MOF-246 expected from the crystal structure is not large enough to permit the diffusion of DMF molecules.

The interpenetration process seems to be sensitive to the functionality of MOFs. The PXRD pattern of the isostructure of MOF-123 having Br functionalities (Zn_7O_2(2-bromo-1,4-benzenedicarboxylate)$_5$) did not change by heating, which is indicative of no interpenetration. Considering that the NO_2 functional group is potentially coordinative, less-coordinated Zn ions in the transient states can be stabilized by the coordination of NO_2 groups of NBD-*ab* linkers. The rotation of the phenylene ring of NBD-*ab* linkers against the *ab* plane might also be related to the stabilization process.

As the gradual interpenetration requires changes in the porosity of MOF-123, gas adsorption measurements were performed to probe the porosity features related to the forward and reverse transformation in bulk samples. The profile of N_2 isotherm of MOF-123 measured at 77 K is classified as a typical type I isotherm (Figure 3b). The Brunauer–Emmett–Teller (BET) and Langmuir surface areas of MOF-123 are calculated to be 1200 and 1340 $m^2 g^{-1}$, respectively. The maximum N_2 uptake in the selected intermediate samples, *a* and *b*, were almost the same as that of MOF-123. This most likely indicates that the volume created by the removal of DMF was compensated by the interpenetration. However, once a large part of the framework became MOF-246 upon further progression of the interpenetration, the amount of N_2 uptake dropped, and finally MOF-246 did not take up N_2.

Interestingly, the intermediate phases heated at various temperatures under vacuum showed rather complex isotherms (note that the activation temperature here is not the same as that for the PXRD measurement because the latter samples are prepared under ambient pressure). The characteristic feature of the isotherms was a sharp step at approximately $P/P_0 = 0.1$ and a significant hysteresis loop for the intermediates *a*, *b*, and *c* in Figure 3b. This type of isotherm for the intermediate phases can be seen for the MOFs exhibiting a dynamic structural change in frameworks with various origins, such as a gate-opening mechanism.[14] Similar steps with a hysteresis loop were also observed by high-pressure isotherms of CH_4 and CO_2 (Supporting Information, Figure S10), but these were not the case for MOF-123.

Noteworthy is the fact that the transformation is reversible and can be cycled many times. Addition of DMF to the interpenetrating crystals of MOF-246 initiates the transformation back to MOF-123 without losing crystallinity and with the regeneration of porosity (Supporting Information, Figure S11). In fact, this process was repeated five times by heating the crystals of MOF-123 to remove DMF and to trigger the formation of MOF-246, which upon the addition of DMF transforms back to MOF-123 (Figure 4a). It is worth noting the transformation was observed within 10 min by the addition of only a tiny amount of DMF (0.25 mL) to the MOF sample (100 mg) at 180 °C and that the transformation was completed after heating for 150 min. To verify that the dissolution and re-crystallization of the MOFs was not taking place, we also measured ^{1}H NMR of the supernatant after the completion of the deinterpenetration; however, no NBD linker was detected. Indeed, the gradual incorporation of DMF was also supported by the IR and TGA data for the collected samples (Supporting Information, Figure S11).

The interpenetration and deinterpenetration of MOF-123 is not a simple reversible process. We realized that the N_2 isotherms of an intermediate, which was prepared by the

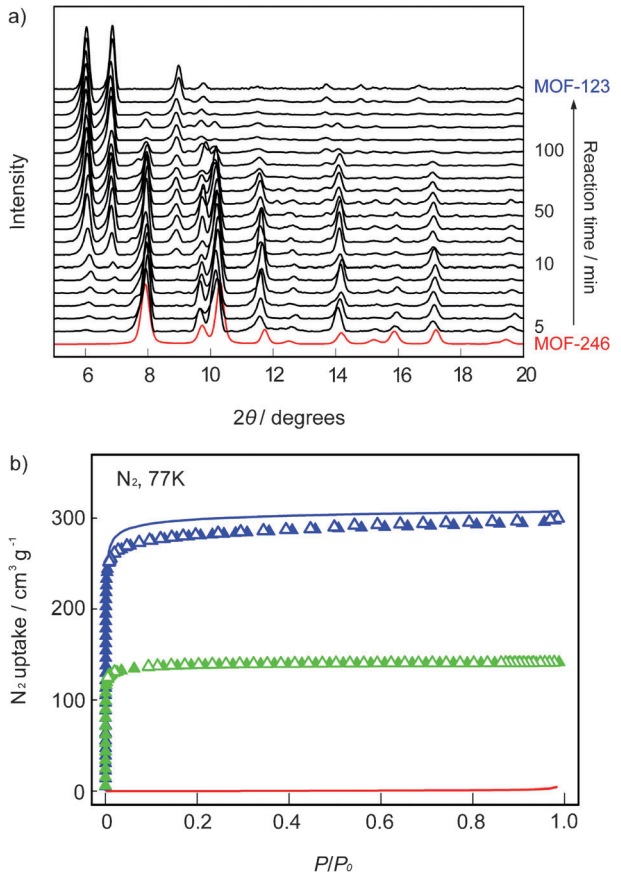

Figure 4. a) PXRD patterns for the deinterpenetration with reaction times. b) N_2 adsorption isotherms (green and blue triangles) for two isolated products during the deinterpenetration. As the reaction proceeds, more nitrogen molecules are adsorbed without hysteresis. Blue and red lines are the adsorption traces of MOF-123 and MOF-246, respectively.

addition of DMF, did not show a hysteresis loop (Figure 4b). This indicates that, in terms of the macroscopic view, the arrangement of NBD linkers in the intermediate form are not the same, although the PXRD patterns of the intermediates in deinterpenetration are nearly identical to those in the interpenetration form (Figures 3a and 4a). This brings up a very important implication that, even if the chemical formula is exactly the same, the heterogeneity of pore structure can be introduced by controlling the arrangement of organic linker in the MOF structure.[15] Although the functionality is critical for the transformation in the present system, a myriad of MOFs with a variety of functionalities remain untested. In this sense, it is conceivable that MOFs with multivariate functionalities (MTV-MOFs) are good candidates to introduce heterogeneity into well-ordered frameworks.

Received: April 17, 2012
Revised: June 8, 2012
Published online: July 17, 2012

Keywords: interpenetration · metal–organic frameworks · porosity · structural transformation · zinc

[1] a) I. A. Baburin, V. A. Blatov, L. Carlucci, G. Ciani, D. M. Proserpio, *J. Solid State Chem.* **2005**, *178*, 2452–2474; b) C. G. Salzmann, P. G. Radaelli, B. Slater, J. L. Finney, *Phys. Chem. Chem. Phys.* **2011**, *13*, 18468–18480.

[2] a) Water structure and science. http://www.lsbu.ac.uk/water/phase.html (accessed June **2012**); b) T. A. Pascal, C. Boxe, W. A. Goddard, *J. Phys. Chem. Lett.* **2011**, *2*, 1417–1420.

[3] a) H. Kim, M. P. Suh, *Inorg. Chem.* **2005**, *44*, 810–812; b) D. J. Tranchemontagne, J. R. Hunt, O. M. Yaghi, *Tetrahedron* **2008**, *64*, 8553–8557; c) H. Kim, S. Das, M. G. Kim, D. N. Dybtsev, Y. Kim, K. Kim, *Inorg. Chem.* **2011**, *50*, 3691–3696; d) J. Yang, J.-F. Ma, S. R. Batten, S. W. Ng, Y.-Y. Liu, *CrystEngComm* **2011**, *13*, 5296–5298.

[4] a) M. Eddaoudi, J. Kim, N. L. Rosi, D. T. Vodak, J. Wachter, M. O'Keeffe, O. M. Yaghi, *Science* **2002**, *295*, 469–472; b) O. Shekhah, H. Wang, M. Paradinas, C. Ocal, B. Schüpbach, A. Terfort, D. Zacher, R. A. Fischer, C. Wöll, *Nat. Mater.* **2009**, *8*, 481–484; c) J. Zhang, L. Wojtas, R. W. Larsen, M. Eddaoudi, M. J. Zaworotko, *J. Am. Chem. Soc.* **2009**, *131*, 17040–17041; d) O. K. Farha, C. D. Malliakas, M. G. Kanatzidis, J. T. Hupp, *J. Am. Chem. Soc.* **2010**, *132*, 950–952; e) S. Bureekaew, H. Sato, R. Matsuda, Y. Kubota, R. Hirose, J. Kim, K. Kato, M. Takata, S. Kitagawa, *Angew. Chem.* **2010**, *122*, 7826–7830; *Angew. Chem. Int. Ed.* **2010**, *49*, 7660–7664; f) D. J. Lun, G. I. N. Waterhouse, S. G. Telfer, *J. Am. Chem. Soc.* **2011**, *133*, 5806–5809; g) J. Kim, S.-T. Yang, S. B. Choi, J. Sim, J. Kim, W. S. Ahn, *J. Mater. Chem.* **2011**, *21*, 3070–3076.

[5] L. Ma, W. Lin, *Angew. Chem.* **2009**, *121*, 3691–3694; *Angew. Chem. Int. Ed.* **2009**, *48*, 3637–3640.

[6] Y. Takashima, V. M. Martínz, S. Furukawa, M. Kondo, S. Shimomura, H. Uehara, M. Nakahama, K. Sugimoto, S. Kitagawa, *Nat. Commun.* **2011**, *2*, 168.

[7] T. K. Maji, R. Matsuda, S. Kitagawa, *Nat. Mater.* **2007**, *6*, 142–148.

[8] a) M. Fujita, F. Ibukuro, H. Hagihara, K. Ogura, *Nature* **1994**, *367*, 720–723; b) K. Yamashita, M. Kawano, M. Fujita, *J. Am. Chem. Soc.* **2007**, *129*, 1850–1851; c) A. Hori, K. Yamashita, M. Fujita, *Angew. Chem.* **2004**, *116*, 5126–5129; *Angew. Chem. Int. Ed.* **2004**, *43*, 5016–5019.

[9] J.-P. Zhang, Y.-Y. Lin, W.-X. Zhang, X.-M. Chen, *J. Am. Chem. Soc.* **2005**, *127*, 14162–14163.

[10] Crystal and refinement information: MOF-123: monoclinic, *C*2/*m*, $a = 18.7789(11)$, $b = 17.8270(11)$, $c = 14.3603(9)$ Å, $\beta = 93.827(1)°$, $V = 4796.7(5)$ Å^3, $T = 173$ K, $M_r = 1681.35$, $Z = 2$, $d_{calc} = 1.164$ g cm^{-3}, μ(MoKα) = 1.785 mm^{-1}, $R_{int} = 0.0414$, $R1$-[$I > 2\sigma(I)$] = 0.0516; w$R2$(all data) = 0.1428, 5050 unique reflections; MOF-246: monoclinic, *C*2/*m*, $a = 16.177(3)$, $b = 18.174(4)$, $c = 9.827(2)$ Å, $\beta = 118.965(4)°$, $V = 2527.7(9)$ Å^3, $T = 153$ K, $M_r = 1535.16$, $Z = 2$, $d_{calc} = 2.017$ g cm^{-3}, μ(MoKα) = 3.373 mm^{-1}, $R_{int} = 0.0878$, $R1[I > 2\sigma(I)] = 0.0941$, w$R2$(all data) = 0.2925, 3269 unique reflections. For details, see the Supporting Information. CCDC 851175 and CCDC 851176 contain the supplementary crystallographic data for this paper. These data can be obtained free of charge from The Cambridge Crystallographic Data Centre via www.ccdc.cam.ac.uk/data_request/cif.

[11] D. J. Darensbourg, J. R. Wildeson, J. C. Yarbrough, *Inorg. Chem.* **2002**, *41*, 973–980.

[12] a) Q.-R. Fang, G.-S. Zhu, M. Xue, Q.-L. Zhang, J.-Y. Sun, X.-D. Guo, S.-L. Qiu, S.-T. Xu, P. Wang, D.-J. Wang, Y. Wei, *Chem. Eur. J.* **2006**, *12*, 3754–3758; b) M. O'Keeffe, O. M. Yaghi, *Chem. Rev.* **2012**, *112*, 675–702.

[13] E. V. Alexandrov, V. A. Blatov, A. V. Kochetkov, D. M. Proserpio, *CrystEngComm* **2011**, *13*, 3947–3958.

[14] a) R. Kitaura, K. Fujimoto, S. Noro, M. Kondo, S. Kitagawa, *Angew. Chem.* **2002**, *114*, 141–143; *Angew. Chem. Int. Ed.* **2002**,

41, 133 – 135; b) S. Bourrelly, P. L. Llewellyn, C. Serre, F. Millange, T. Loiseau, G. Férey, *J. Am. Chem. Soc.* **2005**, *127*, 13519 – 13521; c) K. Uemura, Y. Yamasaki, Y. Komagawa, K. Tanaka, H. Kita, *Angew. Chem.* **2007**, *119*, 6782 – 6785; *Angew. Chem. Int. Ed.* **2007**, *46*, 6662 – 6665; d) H. J. Park, M. P. Suh, *Chem. Commun.* **2010**, *46*, 610 – 612; e) S. Henke, R. A. Fischer, *J. Am. Chem. Soc.* **2011**, *133*, 2064 – 2067.

[15] K. M. Choi, H. J. Jeon, J. K. Kang, O. M. Yaghi, *J. Am. Chem. Soc.* **2011**, *133*, 11920 – 11923.

